INSTITUT FÜR PLASMAPHYSIK

GARCHING BEI MÜNCHEN

THEORY OF THE RESONANCE PROBE

by

H.K. Wimmel

IPP/6/11 December 1963

Die nachstehende Arbeit wurde im Rahmen des Vertrages zwischen dem Institut für Plasmaphysik GmbH und der Europäischen Atomgemeinschaft über die Zusammenarbeit auf dem Gebiete der Plasmaphysik durchgeführt.

ABSTRACT

1. The theory of the resonance probe by Ichikawa and Ikegami [5] is critically reviewed and found unsatisfactory for three reasons. First, because it neglects the resonance increase of the rf field at $\omega_{res} < \omega_p$ produced by the plasma-sheath inhomogeneity. Second, since it uses an improper normalization of the rf field amplitude. Third, because it yields a resonance frequency which, for given electron density, is independent of the sheath thickness, in contradiction to experiments. [2,3]

2. The dc electron current as a function of frequency is computed for two different one-dimensional models of the resonance probe (radius R, dc voltage V, rf amplitude δV, sheath thickness δ) that take the rf resonance mentioned above into account. The rf field is derived from linearized plasma equations, with the dielectric constant of the sheath equated to 1. The plasma equations neglect Landau damping, but contain a "collision frequency" ν that must be put of the order of ω_p in order to obtain reasonable results. The dc current is derived by summing over all electrons having positive kinetic energy at the probe surface. Here, collisions are neglected, and the time of flight is estimated from the unperturbed electron velocities. Both models yield a dc resonance with $\omega_{res} < \omega_p (\delta/R)^{1/2} \ll \omega_p$ being dependent on r_D/R, ν/ω_p, and eV/kT_e, but nearly independent of $e\delta V/kT_e$. For $\omega \ll \omega_{res}$ and $\omega \gg \omega_{res}$ the correct limiting values of the dc current are reproduced. There is no resonance at $\omega = \omega_p$ at all. These results are incompatible with the ones by Ichikawa and Ikegami [5], but are in good qualitative agreement with experiments. [2,3]

CONTENTS

I. INTRODUCTION

The resonance probe, or radio-frequency probe, has been proposed as a new device for measuring plasma density, temperature, and collision frequency.[1,5] The rf probe has applied to it a dc voltage V - usually negative in sign - and an additional rf voltage of variable frequency ω and of amplitude δV. Preferably the dc current to the probe is measured.

Experimental results, so far, or not in complete agreement.[1-4] However, for $V<0$ the following general observations seem valid:

1. At low frequencies, $\omega \ll \omega_p$, the dc electron current assumes a limiting value larger than the static, or Langmuir, current.

2. At a resonance frequency $\omega = \omega_{res}$ below the plasma frequency ω_p a resonance peak of the dc current is observed.

3. At frequencies $\omega > \omega_{res}$ the dc current approaches the unperturbed static current.

4. At times, secondary peaks at lower or higher frequencies appear.

5. For a certain value of V the peak hight of the dc current reaches a maximum.[2,4] The peak height increases monotonically with δV.

6. For V becoming more negative the resonance frequency increases.[2,3] This proves that the resonance frequency is different from the plasma frequency.

7. There are indications that the resonance effect will disappear for probe diameters smaller than the Debye length.[2]

We turn to existing theories of the rf probe. The low-frequency limit for the dc electron current density is:[1]

1) $$j_Q = j_S \cdot I_0(\delta\eta) \quad ,$$

where $\delta\eta = e\,\delta V/kT_e$, I_0 is the modified Bessel function of zeroth order, and j_s is the static electron current density:

$$j_s = n_0 e \,(kT_e/2\pi m_e)^{1/2} \exp(-\eta) \,, \tag{2}$$

with $\eta = -eV/kT_e$. We shall call j_Q the "quasistatic current density".

A theory of the dc current for $\omega \approx \omega_p$ has been given by Ichikawa and Ikegami.[5] Their analysis consists of two parts, A and B, say. Part A concerns the rf field and its effect upon the electron velocity distribution f(v). A plane condenser with idealized properties is thought immersed in a homogeneous plasma. The two plates are situated at x=-L and x=+L and neither absorb nor emit particles. Even though, in experiments, the rf probe is always operated with a fixed amplitude of the rf voltage as ω is varied, in the theory by Ichikawa and Ikegami it is instead the homogeneous rf displacement current between the plates ("external rf field") for which a constant amplitude independent of ω is assumed.[5a] The dc voltage between the plates is put equal to zero, i.e. the dc field, the dc current, and the dc sheath are neglected at this stage. With these assumptions the perturbed f(v) at the midplane of the condenser is determined from the linearized Boltzmann-Vlasov (B.V.) equation. - Subsequently, in part B, the dc current is derived. This is done by considering, in addition, an inhomogeneous plasma model which consists of a plane probe, an adjacent dc sheath of thickness L, and a (homogeneous) plasma region. In this model, the total voltage drop, $V_{tot} = V + \delta V \cdot \sin(\omega t)$, is assumed to be confined to the sheath. In order to derive the dc current to the probe the homogeneous model is mapped upon the inhomogeneous one. Thus, the right-hand plate of part A is identified with the probe surface of part B. The half plate distance L is reinterpreted as a "penetration depth" within which the "external rf field" is shielded out by charge accumulations of the plasma. The midplane of the condenser is taken as the plasma-sheath boundary, and the perturbed f(v) of part A as the velocity distribution at the plasma-sheath boundary. The dc current is calculated as the time average of $\int v f(v) dv$ over all electrons with $v>0$ that can reach the probe. Since in determining those the transit time through the sheath is neglected, only the voltage drop through the sheath is of interest; the E-field itself can be left undetermined.

Results in analytical form for the dc current are obtained. Characteristically, the resonance frequency depends only on ω_p and the collision frequency ν. The reason for this is that, in part A, the dc sheath has been omitted. For $\nu \to 0$ there follows $\omega_{res} \to \omega_p$. For a partially ionized plasma, the parameter L enters into the expression for the peak height of the dc current, but not into that for the half-width. For a fully ionized plasma, the opposite holds.

However, the analysis of Ichikawa and Ikegami appears unsatisfactory for the following reasons:

1. The spatial variation of the external rf field E_{ext} ought to depend only on geometrical factors, not on the charge density of the plasma (shielding effect). It is rather the total E-field that will be affected by shielding. Hence, the quantity L has not been sufficiently well defined to permit a meaningful comparison of experimental and theoretical peak heights or half-widths.

2. The external rf field E_{ext}, rather than the total rf field $(E + E_{ext})$, has been normalized such that its path integral yields the rf voltage.[5a] It is this improper normalization that provides for at least part of the resonance increase of the total rf field - and therefore of the dc current - near ω_p.

3. In part A, an rf voltage amplitude of $(2\delta V)$ occurs between x=-L and x=+L, whereas in part B, Eqs. (18) and (19), only an rf voltage amplitude of δV is considered between x=0 and x=+L. This inconsistency may lead to overestimating the dc current.

4. The theory of Ichikawa and Ikegami neglects the resonance increase of the rf field found by several authors [3,8,9,10] (see below) to occur at frequencies below ω_p on account of the plasma-sheath inhomogeneity.

5. Ichikawa and Ikegami cannot account for the dependence of ω_{res} on the sheath thickness at fixed electron density, which has been confirmed experimentally. [2,3]

Under the circumstances it seems worthwhile to investigate different models of the resonance probe.

In another paper Ichikawa has also considered the effect of a nonvanishing transit time through the sheath. [6]

A novel interpretation of the resonance effect has been proposed by Mayer [3] and Harp. [8] These authors consider that taking into account the positive ion sheath at the probe surface is essential in order to obtain the resonance effect. Mayer considers a plane plasma condenser and explaines its rf behavior in terms of a three-slab dielectric. The effective dielectric constant has a resonance at

$$\omega_{res} \approx \omega_s \equiv \omega_p \left(\frac{2s}{p+2s} \right)^{1/2} , \tag{3}$$

where p and s denote the plasma and sheath diameters. A similar formula was derived by Vandenplas and Gould in a different connection. [7] Harp has considered the same model in a spherical geometry. [8] In the theoretical sections of these papers only the rf field was considered. The dc current increase was not derived. It was merely assumed that at the resonance of the effective dielectric constant also the dc current would show a resonance peak.

Indeed, a numerical evaluation of the rf voltage amplitudes and phases from the Mayer model shows the following. Be δV_p and δV_s the rf voltage amplitudes in the plasma and in the sheath, respectively, and $\varphi = \varphi_p - \varphi_s$. For $\omega < \omega_{res}$ we find $\delta V_p + \delta V_s \approx \delta V$, as $\delta V_p \ll \delta V_s$, even though $\varphi \approx -\frac{\pi}{2}$. For $\omega > \omega_{res}$ again $\delta V_p + \delta V_s \approx \delta V$, but, depending on ω_{res}/ω_p, the reason for this varies. If $\omega_{res} \ll \omega_p$, then $\delta V_p \gg \delta V_s$ for $\omega > \omega_{res}$, while φ can vary considerably. If $\omega_{res} \lesssim \omega_p$, then $|\varphi| \ll 1$ for $\omega > \omega_{res}$, while $\delta V_p \sim \delta V_s$. Now, the resonance occurs at $\omega = \omega_{res}$, such that $\delta V_p \sim \delta V_s$ and simultaneously $-\pi < \varphi < -\frac{\pi}{2}$, whence $\delta V_p + \delta V_s > \delta V$. It follows that electrons transversing this field may gain or lose more energy than $e\delta V$. Therefore a dc resonance is to be expected. The results presented in Section VI show that this consideration is correct.

That the Mayer model yields values of the rf field that are qualitatively correct has been shown by beam experiment [9] and by detailed theoretical analysis. [10] As Ichikawa and Ikegami [5] neglect this resonance increase of the rf field connected with the plasma-sheath inhomogeneity, they may miss the very mechanism responsible for the dc resonance.

Clearly, the condenser model of the rf probe neglects the x-dependence of the rf field in the homogeneous plasma. Hence we shall treat two models, viz., Model 1, which is a generalized condenser model that takes into account also the k-dependence of the plasma dielectric constant, and Model 2, which resembles Mayer's model in assuming $\varepsilon = \varepsilon(\omega)$. While Mayer's original model is symmetric in x, ours are both asymmetric, with only one condenser plate and one sheath present. (For details see below.) For both models the dc current is computed as a function of the radio frequency ω and of the other parameters.

II. THE DC CURRENT TO THE RF PROBE

We shall do an approximate computation of the dc electron current to an rf probe for negative dc voltage V. The following one-dimensional model (=Model 1) is considered (Fig. 1). Adjacent to the probe there is a perturbed plasma region of diameter R, including a dc sheath of thickness δ. For $x < 0$ the plasma be unperturbed. The parameter R designates the distance from the probe up to which the displacement current is of appreciable magnitude. In the case of a spherical probe, R could be identified with its radius; in the case of a plane probe, R should be chosen of the order of the plate diameter, etc. Clearly, this simplified model is only appropiate for $\delta < R$. The opposite case would definitely require treating the geometry more accurately.

The dc electron current density to the probe is approximately

(4) $$j = j_0 (2\pi)^{-1} \int_0^{2\pi} d\varphi \int_0^{\infty} d\beta_0 \; e^{-\beta_0} \, He(\beta_R) ,$$

where the unperturbed velocity distribution $f_0(v_0)$ of the electrons has been assumed to be Maxwellian. Here j_0 is the thermal current density of electrons:

(5) $$j_0 = n_0 e \left(kT_e / 2\pi m_e \right)^{1/2} ,$$

$\varphi = \omega t_0$ is the rf phase at t_0, the time at which an electron passes through $x=0$ from left to right, β_0 and β_R are its kinetic energies in units of kT_e at $x=0$ and $x=R$, and $He(x)$ is the Heaviside step function, i.e.,

$$He(x) = \begin{cases} 0 \\ 1 \end{cases} \text{for } x \lessgtr 0 .$$

The approximation in Eq.(4) consists in assuming that all those and only those electrons with $\beta_R > 0$ will actually reach the probe. This is a good approximation for δV and ω sufficiently small, and for particle speeds sufficiently large, i.e., if the total field an electron sees during his passage to the probe is sufficiently close to being a monotonic function of $x(t)$. From conservation of energy there follows, if collisions are neglected,

$$(6) \qquad \beta_R = \beta_0 - \eta + (e/kT_0)\int_0^R E_w[x, t(t_0, x)]\, dx ,$$

with $\eta = -eV/kT_e$, E_w the rf field, and t = time. Here and in the following the electron charge is put equal to $(+e)$.

For simplicity we determine t as if the electron speeds were constant in time, i.e., we put

$$(7) \qquad t = t_0 + x/v_0 .$$

In the perturbed plasma region this is a good approximation for most electrons, if the rf field is sufficiently small. In the sheath it is justified for those electrons for which the time of flight through the sheath is not longer than half the rf period. An estimate using the Langmuir-Childs law for the sheath thickness δ shows that for an electron with critical v_0 , i.e., such that $\beta_0 = \eta$, the time of flight is sufficiently short, if $\omega \leqq \omega_p$ and $\eta < 10$. For electrons so slow that their transit time amounts to many half-periods, it is expected that the errors made for electrons of comparable v_0 will cancel out. In an intermediate v_0-range, use of Eq.(7) may lead to a certain systematic error in the result.

We shall derive the rf field in Sections III, IV, and V, and approximate it by a two-step, resp. three-step, function of the form:

$$(8) \qquad E_w(x, t) = (\delta V/R)[X_m \cos(\omega t) + Y_m \sin(\omega t)]$$

$$\text{for} \quad R_m \leqq x < R_{m+1} , \quad m = 1, 2, 3 .$$

The x- and φ- integrations can now be carried out, and the result for the dc current is, by straight-forward analysis:

$$j = j_S \left\{ 1 + \int_0^\infty d\beta_0 \; e^{-a} \, \mathrm{sgn}(-a) \, G\left(\left|\frac{a}{b}\right|\right) \right\} , \tag{9}$$

with

$$G(x) = \begin{cases} \pi^{-1} \arccos x & \text{for } 0 \leqq x \leqq 1 \\ 0 & \text{for } 1 < x < \infty \end{cases} \tag{10}$$

$$a = \beta_0 - \eta , \tag{11}$$

$$b = (b_1^2 + b_2^2)^{1/2} , \tag{12}$$

$$b_1 = (\delta\eta/\chi_R) \sum_{n=1}^{3} \left[X_n (\sin\chi_{n+1} - \sin\chi_n) - Y_n (\cos\chi_{n+1} - \cos\chi_n) \right] , \tag{13}$$

$$b_2 = -(\delta\eta/\chi_R) \sum_{n=1}^{3} \left[Y_n (\sin\chi_{n+1} - \sin\chi_n) + X_n (\cos\chi_{n+1} - \cos\chi_n) \right] , \tag{14}$$

where

$$\chi_n = (R_n \omega / r_D \omega_p)(2\beta_0)^{-1/2} , \tag{15}$$

$$\chi_R = (R \omega / r_D \omega_p)(2\beta_0)^{-1/2} , \tag{16}$$

$$\delta\eta = (e\delta V / kT_e) , \tag{17}$$

(18) $$r_D = (kT_e/4\pi n_0 e^2)^{1/2} \quad , \quad \omega_p = (4\pi n_0 e^2/m_e)^{1/2} .$$

The field coefficients X_m, Y_m, and the distances R_n will be given in Sections IV and V.

III. THE RF FIELD IN A HOMOGENEOUS PLASMA

To prepare for the derivation of the rf field in the inhomogeneous plasma models, the rf field that is produced in a homogeneous plasma by an ideal condenser of the type considered by Ichikawa and Ikegami [5] is calculated (Fig. 2). In essence this homogeneous model has been described in Section I. But for convenience the plates now are situated at x=0 and x=L, rather than at x=-L and x=+L as in Ref. 5. For simplicity we neglect Landau damping and replace the linearized B.V. equation by the adiabatic moment equations for electrons:

(19) $$\frac{\partial n}{\partial t} + n_0 \frac{\partial v}{\partial x} = 0 ,$$

(20) $$\frac{\partial v}{\partial t} = \frac{e}{m_e} E - \frac{\gamma\theta}{m_e n_0} \frac{\partial n}{\partial x} - \nu v ,$$

(21) $$E = E_i + E_a ,$$

(22) $$\frac{\partial E_i}{\partial x} = 4\pi e n ,$$

where n, v, E_i, E_a are small perturbations, $\theta = kT_e$, $\gamma = c_p/c_v = 3$, ν= collision frequency. The displacement current E_a is put equal to zero outside the condenser:

(23) $$E_a = E_{a0} \sin(\omega t) \int_{-\infty}^{+\infty} (2\pi i k)^{-1} \left(1 - e^{-ikL}\right) e^{ikx} \, dk ,$$

with E_{a0} to be determined from

(24) $$\int_0^L E \, dx = \delta V \sin(\omega t + \alpha) .$$

By the usual Fourier transform method there follows the dielectric constant

(25) $$\varepsilon(k, \omega) = 1 - \left[\frac{\omega(\omega + i\nu)}{\omega_p^2} - \gamma (k r_D)^2 \right]^{-1}$$

and the rf field

(26) $$\mathbf{E}(x,t) = E_0 - E_L ,$$

where

(27) $$E_0(x,t) = E_{ao}\,\mathrm{sgn}(x)\Big\{\Big[\big(\tfrac{1}{2}+c'\big)\sin(\omega t) - c''\cos(\omega t)\Big] + e^{-|k''x|}\Big[c'\sin(|k'x|-\omega t) + c''\cos(|k'x|-\omega t)\Big]\Big\} ,$$

and $E_L(x,t)$ is obtained by replacing x by (x-L) in $E_0(x,t)$.
The coefficients are:

(28) $$c' = \frac{\omega_p^2(\omega^2-\omega_p^2)}{2[(\omega^2-\omega_p^2)^2+(\nu\omega)^2]} ,$$

(29) $$c'' = \frac{-\omega_p^2\,\nu\omega}{2[(\omega^2-\omega_p^2)^2+(\nu\omega)^2]} ,$$

(30) $$k' = \left(\frac{m_e}{\gamma\theta}\right)^{1/2}\left\{\left[\left(\frac{\omega^2-\omega_p^2}{2}\right)^2+\left(\frac{\nu\omega}{2}\right)^2\right]^{1/2} + \frac{\omega^2-\omega_p^2}{2}\right\}^{1/2} ,$$

(31) $$k'' = \left(\frac{m_e}{\gamma\theta}\right)^{1/2}\left\{\left[\left(\frac{\omega^2-\omega_p^2}{2}\right)^2+\left(\frac{\nu\omega}{2}\right)^2\right]^{1/2} - \frac{\omega^2-\omega_p^2}{2}\right\}^{1/2} .$$

We see that the rf field is screened out within a few Debye lengths from the condenser plates, if $\omega \ll \omega_p$. For $\omega \approx \omega_p$ the rf field is virtually homogeneous, as it is for $\omega \gg \omega_p$. In a certain frequency range $\omega > \omega_p$ there are also running wave terms contributing to $\mathbf{E}$.

IV. THE RF FIELD OF MODEL 1

In this section the rf field coefficients X_n, Y_n, and the characteristic distances R_n for Model 1 will be derived.

Consider again the one-dimensional model of Fig. 1. We shall use the Langmuir-Childs law to define the dc sheath thickness

(32) $$\delta \equiv R - R_\delta = 1.25\, r_D\, \eta^{3/4} \left(T_i/T_e\right)^{1/4},$$

where the ion current has been equated to the thermal current. This seems a reasonable approximation for a plane probe and for moderate values of η. For spherical and cylindrical probes and/or large values of η a better approximation is required.

We shall also need the thickness δ_v of the "effective sheath", which is that part of the dc sheath where the local plasma frequency is smaller than the applied frequency ω. From the Langmuir-Childs law we have, for $\omega < \omega_p$:

(33a) $$\delta_v \equiv R - R_v = \delta - 1.25\, r_D \left| \ln\left(\frac{\omega_p}{\omega}\right)^2 \right|^{3/4} \left(T_i/T_e\right)^{1/4},$$

if the quantity on the right-hand side is positive, and

(33b) $$\delta_v = 0$$

otherwise. For $\omega \geqq \omega_p$ we have

(33c) $$\delta_v = \delta .$$

A third quantity needed is the rf screening distance

(34) $$\delta_s \equiv R - R_s = \delta_v + |k''|^{-1} .$$

The rf field is now obtained in the following way. The displacement current is written as

(35) $$E_a = E_{a0} \sin(\omega t) \int_{-\infty}^{+\infty} (2\pi i k)^{-1} \left(1 - e^{-ikR}\right) e^{ikx}\, dk,$$

with E_{a0} to be determined from

(36) $$\int_0^R E\, dx = \delta V \sin(\omega t + \alpha) .$$

Within the effective sheath, $R_v < x \leqq R$, we put $E = E_a$. The remaining plasma, $0 \leqq x < R_v$ is considered homogeneous, with density n_0. To obtain the rf field within this region we first use Eq. (26), but with L replaced by R_v. The E-field thus obtained is further adapted to the model of Fig. 1. Since the discontinuity of E_a at x=0 represents a geometrical cut-off of the displacement current, not the presence of a second probe, the inhomogeneous part (i.p.) is dropped from E_0, i.e.,

(37) $$E = E_0^{h.p.} - E_v ,$$

where the abbreviation h.p. means "homogeneous part", and E_v is obtained by replacing x by $(x-R_v)$ in the expression for E_0, Eq. (27). In order for Eq. (8) to be applicable the rf field of Eq. (37) is approximated by a multistep function. Two cases must be distinguished.

Case 1: $\omega \leqq \omega_p$, $R_s \geqq 0$. We put

(38a) $$E = E_0^{h.p.} - E_v^{h.p.} \quad \text{for } 0 \leqq x \leqq R_s$$

and

(38b) $$E = E_0^{h.p.} - E_v^{h.p.} - (R_v - R_s)^{-1} \int_0^{R_v} E_v^{i.p.}\, dx$$

$$\text{for } R_s < x \leqq R_v .$$

Case 2: Either $\omega \leqq \omega_p$, $R_s < 0$,

or $\omega > \omega_p$.

Here we put

(39) $$E = E_0^{h.p.} - E_v^{h.p.} - R_v^{-1} \int_0^{R_v} E_v^{i.p.}\, dx$$

for $0 \leqq x \leqq R_v$.

In the following the field coefficients and characteristic lengths are listed.

Case 1.

$R_1 = 0$	$X_1 = -2c'' N$	$Y_1 = (1+2c')N$
$R_2 = R_s$	$X_2 = BN$	$Y_2 = AN$
$R_3 = R_v$	$X_3 = 0$	$Y_3 = N$
$R_4 = R$		

with

$$N = -\left\{\left[\frac{R_s}{R}(1+2c') + \frac{R_v - R_s}{R} A + \left(1 - \frac{R_v}{R}\right)\right]^2 + \left[\frac{R_s}{R}(-2c'') + \frac{R_v - R_s}{R} B\right]^2\right\}^{-1/2} ,$$

$$A = \sum_{n=1}^{2} (A_n \cos \delta_n - B_n \sin \delta_n) ,$$

$$B = \sum_{n=1}^{2} (A_n \sin \delta_n + B_n \cos \delta_n) ,$$

$$A_1 = 1 + 2c' - \frac{k''(c'k'' - c''k')}{k'^2 + k''^2} ,$$

$$A_2 = e^{-k'' R_v} \frac{k''(c'k'' - c''k')}{k'^2 + k''^2} ,$$

$$B_1 = -2c'' + \frac{k''(c'k' + c''k'')}{k'^2 + k''^2} ,$$

$$B_2 = -e^{-k'' R_v} \frac{k''(c'k' + c''k'')}{k'^2 + k''^2} ,$$

$$\delta_1 = 0 ,$$

$$\delta_2 = -k' R_v .$$

Case 2.

$R_1 = 0$	$X_1 = BN$	$Y_1 = AN$
$R_2 = R_v$	$X_2 = 0$	$Y_2 = N$
$R_3 = R$	$X_3 = 0$	$Y_3 = 0$
$R_4 = R$		

with

$$N = -\left\{\left[\frac{R_v}{R}A + \left(1 - \frac{R_v}{R}\right)\right]^2 + \left[\frac{R_v}{R}B\right]^2\right\}^{-1/2} ,$$

$$A_1 = 1 + 2c' - \frac{c'k'' - c''k'}{R_v(k'^2 + k''^2)} ,$$

$$A_2 = e^{-k''R_v} \frac{c'k'' - c''k'}{R_v(k'^2 + k''^2)} ,$$

$$B_1 = -2c'' + \frac{c'k' + c''k''}{R_v(k'^2 + k''^2)} ,$$

$$B_2 = -e^{-k''R_v} \frac{c'k' + c''k''}{R_v(k'^2 + k''^2)} .$$

The variables A, B, δ_1 , δ_2 satisfy the same equations as in Case 1.

V. THE RF FIELD OF MODEL 2

For the purpose of comparison the dc current of a simpler model, in essence proposed by Mayer [3] and Harp [8], has also been computed. The model (=Model 2) is shown in Fig. 3. R_δ is again computed from Eq. (32). In the sheath, $R_\delta < x \leqq R$, we put again $E = E_a$, with E_a again given by Eq. (35). In the perturbed plasma, $0 \leqq x \leqq R_\delta$, the dielectric constant

$$\varepsilon(\omega) = 1 - \omega_p^2 / (\omega^2 + i\nu\omega) \tag{40}$$

is used. After applying the normalization of Eq. (36), the following field coefficients X_n, Y_n, and characteristic distances R_n are obtained.

$R_1 = 0$	$X_1 = -2c'' N$	$Y_1 = (1 + 2c') N$
$R_2 = R_\delta$	X_2 not needed	Y_2 not needed
$R_3 = R_\delta$	$X_3 = 0$	$Y_3 = N$
$R_4 = R$		

with c', c'' again obtained from Eqs. (28) and (29), and

$$N = -\left\{ \left[2c' \frac{R_\delta}{R} + 1 \right]^2 + \left[2c'' \frac{R_\delta}{R} \right]^2 \right\}^{-1/2} .$$

VI. NUMERICAL RESULTS

From the two models numerical results for the dc electron current as a function of frequency have been derived. The other parameters were assigned these values:

$$r_s/R = 0.1; \quad 0.01$$

$$\nu/\omega_p = 0.6; \quad 0.2$$

$$\eta = 3; \ 4; \ 5; \ etc. \ldots; \ 12$$

$$\delta\eta = \begin{cases} 1.2; \quad 1.8; \quad 2.4 & \text{for } \nu/\omega_p = 0.6 \\ 0.75; \quad 1.125; \quad 1.5 & \text{for } \nu/\omega_p = 0.2 \end{cases}$$

$$T_i/T_e = 1.$$

The two models leave out of consideration trapped electrons or ones repeatedly reflected by the field before they eventually either reach the probe or leave the perturbed plasma region. Accordingly, the rf amplitudes $\delta\eta$ were chosen such that slow electrons, with $\beta_0 \ll 1$, should not contribute to the dc current. For $3 \leq \eta \leq 12$ this was found to be valid, while for $\eta = 1$ and 2 the values of $\delta\eta$ were still too large for the restriction to hold. Consequently, the results for $\eta = 1$ and 2 were discarded as probably invalid.

The results for $r_s/R = 0.1$ and $\nu/\omega_p = 0.6$ are shown, for Model 1 in Figs. 5 to 11, and for Model 2 in Figs. 12 to 18. For these values of the parameters the results of the two models are rather similar. In either case the first 4 figures show plots of the dc current density versus the frequency for $\eta = 3; 6; 9; 12$. The second 3 figures show the resonance frequency, the half-widths, and the quotient of the peak current over the static current, all versus η. For obvious reasons a low-frequency half-width and a high-frequency half-width have been distinguished, their definitions being explained by Fig. 4.

From Figs. 5 to 18 it is seen that, at low frequencies, the correct asymptotic limit, as given by Eq. (1), is reached by the dc current, while at $\omega > \omega_{res}$ the static current density is approached. The small secondary maxima at $\omega > \omega_{res}$ are probably due to the crude geometry of the two models.

The reduction of the dc current to the static value for $\omega > \omega_{res}$ rests on two effects. First, the relative transit time, in units of the oscillation period, increases with ω, an effect investigated by Ichikawa [6], but effective only for $\omega > \omega_p$. More important is the increase of the absolute transit time that is caused by the penetration of the rf field into the plasma at sufficiently high frequencies. Ichikawa and Ikegami mention this effect for $\omega > \omega_p$. [5] However, a numerical analysis of the rf field of Model 2 shows that rf field penetration is important for $\omega > \omega_{res}$, even if $\omega_{res} \ll \omega_p$. Indeed, for $\omega > \omega_{res}$ one obtains $\delta V_p > \delta V_s$ (for notation compare Section I, p. 4), i.e., the major rf voltage drop occurs in the plasma, even though still $\delta E_p < \delta E_s$, if $\omega < \omega_p$. Thus, as compared to $\omega < \omega_{res}$ (rf shielding), the absolute transit time is increased by a factor of $R/\delta = \omega_p^2/\omega_s^2$, to become approximately

$$\omega\tau \approx \frac{\omega R}{v_0} \approx \frac{\omega\omega_p}{\omega_s^2}\eta^{3/4}\beta_0^{-1/2} \approx \frac{\omega\omega_p}{\omega_s^2}\eta^{1/4} > 1 ,$$

with $\omega_{res} \approx \omega_s$, and ω_s given by Eq. (3a), below. As the transit time amounts to several oscillation periods, the electrons transversing the perturbed plasma volume see an effective rf voltage amplitude much smaller than δV. As the dc current increment is a very sensitive function of the effective rf voltage, the static dc current is approached comparatively fast for $\omega > \omega_{res}$.

To return to Figs. 5 to 18, the resonance frequency is seen to be nearly independent of $\delta\eta$ (except for lower η), but to increase with η. Always $\omega_{res} < \omega_s < \omega_p$, with

a) $$\omega_s = \omega_p(\delta/R)^{1/2} .$$

Model 1 yields a smaller ω_{res} than Model 2. Similar to ω_{res}, the half-widths depend little on $\delta\eta$. The quotient of the peak current over the static current shows a characteristic η- dependence, with a maximum near $\eta \approx 4$ to 5. The absolute peak current was also computed, but is not shown here. With respect to η the latter showed no maximum in $3 \leqq \eta \leqq 12$. Possibly a maximum would appear for $\eta < 3$, but in this range an improved model would be preferable.

For the other values of the parameters we mention only some characteristic qualitative differences in the results. As ν/ω_p is decreased to 0.2, ω_{res} is increased, (but still $\omega_{res} \leqq \omega_s$), the half-widths are decreased, and the quotient of the peak current over the static current is increased. This is to be expected and holds for both models. As r_D/R is decreased to 0.01, ω_{res} is decreased (more so for Model 1 than for Model 2), so are the half-widths, and the quotient of the peak current over the static current keeps its order of magnitude, but changes its η- dependence.

VII. CONCLUSION

It has been shown that the two models considered exhibit a dc resonance effect of a reasonable order of magnitude, with $\omega_{res} \leqq \omega_s \leqq \omega_p$, ω_{res} being dependent on r_D/R, ν/ω_p, η, and nearly independent of $\delta\eta$. For $\omega < \omega_{res}$ and $\omega > \omega_{res}$ the correct asymptotic values of the dc current are reproduced. At $\omega = \omega_p$ no sign of a resonance is detectable. These results are incompatible with those derived by Ichikawa and Ikegami. [5]

To date, a conclusive comparison of theory and experiment is hampered by an experimental uncertainty, by a factor 2 or 3, of the plasma frequency. There exist, furthermore, difficulties with the experimental determination of the static dc electron current and of the asymptotic values of the dc electron current at small and large frequencies. Nevertheless Peter, Müller, and Rabben [2] appear to have shown definitely that ω_{res} is not a function of the electron density alone, but does depend also on the sheath thickness. In our opinion, Cairns' finding that ω_{res}/ω_p be independent of n_0 does not necessarily follow from his Figure 5. [4] The model of Ichikawa and Ikegami [5] cannot account for this dependence of ω_{res} on the sheath thickness. We conclude that a realistic theory should consider also the sheath in order to obtain the correct resonance frequency. This is done in the Mayer model [3] and in its generalizations used in this paper.

Comparison of the two models used leads to the following conclusion. For $r_D/R = 0.1$ the results from the two models are very similar. For $\omega \ll \omega_p$ one expects the rf sheath to become identical with the dc sheath; hence the Model 2, which identifies the two sheaths for all values of ω, becomes superior at low frequencies. Consequently, for $r_D/R = 0.01$, the value of ω_{res} derived from Model 2 is probably more realistic.

Secondary peaks at $\omega_i = \omega_{res}/i$, i = integer, which have been observed experimentally [2], should be expected also from a more refined theory that would take into account nonlinear dielectric behavior, i.e., generation of harmonics with frequencies $i\omega$.

It turns out that the "collision frequency" ν must be of the order of ω_p in order to obtain reasonable results. That is, the two models considered can explain the resonance effect in a collisionless plasma only, if ν is reinterpreted as an effective damping parameter accounting for Landau damping. It is planned to remedy this by deriving $\varepsilon(\omega, k)$ from the Vlasov equation.

Other aspects of the two models that remain to be improved concern the calculation of the dc sheath thickness, the probe-plasma geometry, the plasma-sheath approximation, the dielectric behavior of an inhomogeneous plasma, and the calculation of the particle orbits.

ACKNOWLEDGMENTS

Stimulating conversations with Professor Dr. A. Schlüter, Dr. G. Müller, and Mr. H. Völk are gratefully acknowledged. The author expresses his thanks to Mrs. G. Hain for advice and help with computer programming.

ADDENDUM

After the numerical calculations and the greater part of the manuscript had been finished three new Research Reports by Ichikawa became known to the author. In the following a few comments are added on these.

In Ref. 11 the theory by Ichikawa and Ikegami [5] is extended to take into account nonvanishing transit times. As can be seen from Figs. 2 to 4 of Ref. 11 the new theory provides for the dc current to approach the static value for $\omega \gg \omega_p$, which was not true for the original theory. [5] However, in contradiction to all experiments known, at $\omega > \omega_p$ there appears a minimum current smaller than the static current. The appearance of $j < j_s$ is also incompatible with the theoretical results presented above in this paper. A clearer interpretation of the "penetration depth" L is now given by Ichikawa, i.e., L = dc sheath diameter. Nevertheless, all objections against the theory by Ichikawa and Ikegami [5] that were raised in Section I still hold and apply also to the extended theory. [11]

In Refs. 12 and 13 nonlinear effects are investigated by the method of van der Pol, Bogoliubov, and Krylov. Numerical results are presented for the peak height of the dc current as a function of various parameters. However, all objections of Section I apply again.

REFERENCES

1. K. Takayama, H. Ikegami, S. Miyazaki, Phys. Rev. Letters 5, 238 (1960).

2. G. Peter, G. Müller, H. H. Rabben, Measurements with the High-Frequency Resonance Probe in a Cesium Plasma, VI. Int. Conf. on Ionization Phen. in Gases, Paris 1963. Lab. Report IPP/2/32 (1963). To be published.

3. H. M. Mayer, Measurements with a "Wide-Band Probe", VI. Int. Conf. on Ionization Phen. in Gases, Paris 1963.

4. R. B. Cairns, Proc. Phys. Soc. 82, 243 (1963).

5. Y. H. Ichikawa, H. Ikegami, Progr. Theoret. Phys. 28, 315 (1962).

5a. Compare Eqs. (5·a) and (5·b) of Ref. 5.

6. Y. H. Ichikawa, Compt. rend. 256, 3434 (1963); VI. Int. Conf. on Ionization Phen. in Gases, Paris 1963.

7. P. E. M. Vandenplas, R. W. Gould, Proc. V. Int. Conf. on Ionization Phen. in Gases, Munich 1961, Vol. 2, p. 1470 (North Holland Pub. Co., Amsterdam 1962).

8. R. S. Harp, A Theory of the Resonance Probe, Microwave Lab., W. W. Hansen Labs. of Physics, Stanford Univ., Stanford, Cal.

9. R. Harp, G. S. Kino, Measurement of Fields in the Plasma Sheath by an Electron Beam Probing Technique, ibid.

10. J. Pavkovich, G. S. Kino, RF Behavior of the Plasma Sheath, ibid.

11. Y. H. Ichikawa, Theoretical Analysis of the Characteristics of Resonance Probe, Research Rept. NUP-63-12, Dept. Physics, College of Sci. and Eng., Nihon University, Tokyo.

12. Y. H. Ichikawa, Research Report NUP-63-14, ibid.

13. Y. H. Ichikawa, Research Report NUP-63-15, ibid.

CAPTIONS OF FIGURES

Fig. 1. Model of the rf probe taking into account the k-dependence of ε (Model 1).

Fig. 2. Ideal plane condenser immersed in a homogeneous plasma.

Fig. 3. Two-slab condenser model of the rf probe (Model 2).

Fig. 4. Definition of two half-widths of the dc resonance curve.

Fig. 5. Dc current of Model 1 versus log (ω/ω_p) for $\eta=3$. Dotted lines: static current and quasistatic limits.

Fig. 6. Dc current of Model 1 versus log (ω/ω_p) for $\eta=6$.

Fig. 7. Dc current of Model 1 versus log (ω/ω_p) for $\eta=9$.

Fig. 8. Dc current of Model 1 versus log (ω/ω_p) for $\eta=12$.

Fig. 9. Log (ω_{res}/ω_p) of Model 1 versus η. Dotted: log (ω_s/ω_p) versus η.

Fig. 10. Log $(\Delta\omega_L/\omega_p)$ of Model 1 versus η. Dotted: log $(\Delta\omega_H/\omega_p)$ versus η.

Fig. 11. j_{res}/j_s of Model 1 versus η. Dotted: j_Q/j_S versus η.

Fig. 12. Dc current of Model 2 versus log (ω/ω_p) for $\eta=3$. Dotted lines: static current and quasistatic limits.

Fig. 13. Dc current of Model 2 versus log (ω/ω_p) for $\eta=6$.

Fig. 14. Dc current of Model 2 versus log (ω/ω_p) for $\eta=9$.

Fig. 15. Dc current of Model 2 versus log (ω/ω_p) for $\eta=12$.

Fig. 16. Log (ω_{res}/ω_p) of Model 2 versus η. Dotted: log (ω_S/ω_p) versus η.

Fig. 17. Log $(\Delta\omega_L/\omega_p)$ of Model 2 versus η. Dotted: log $(\Delta\omega_H/\omega_p)$ versus η.

Fig. 18. j_{res}/j_S of Model 2 versus η. Dotted: j_Q/j_S versus η.

Fig. 1

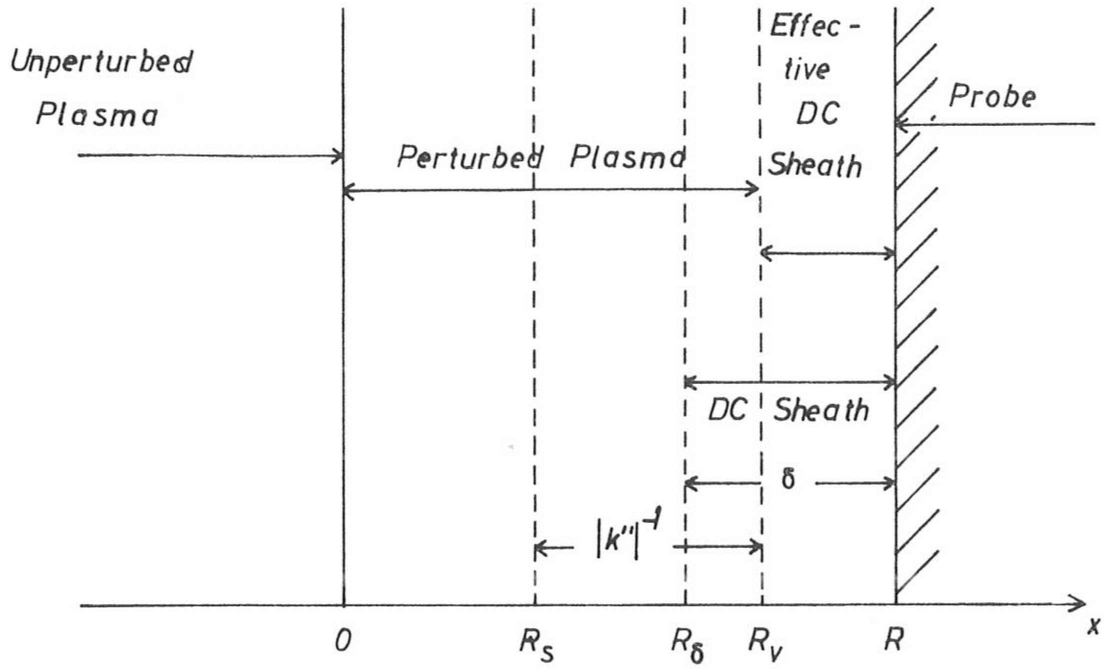
Unperturbed
Plasma
Perturbed Plasma
Effective
DC
Sheath
Probe
DC Sheath
δ
$|k''|^{-1}$
0
R_S
R_δ
R_V
R
x

Fig. 2

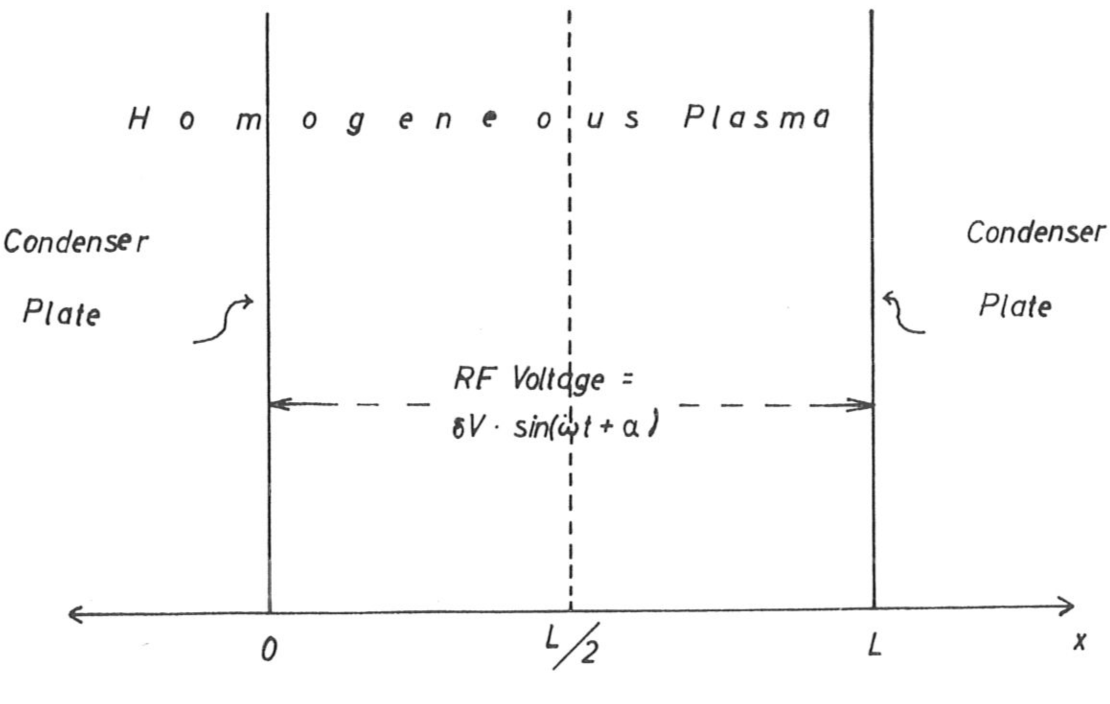
Homogeneous Plasma
Condenser
Plate
Condenser
Plate
RF Voltage =
$\delta V \cdot \sin(\omega t + \alpha)$
0
L/2
L
x

Fig. 3

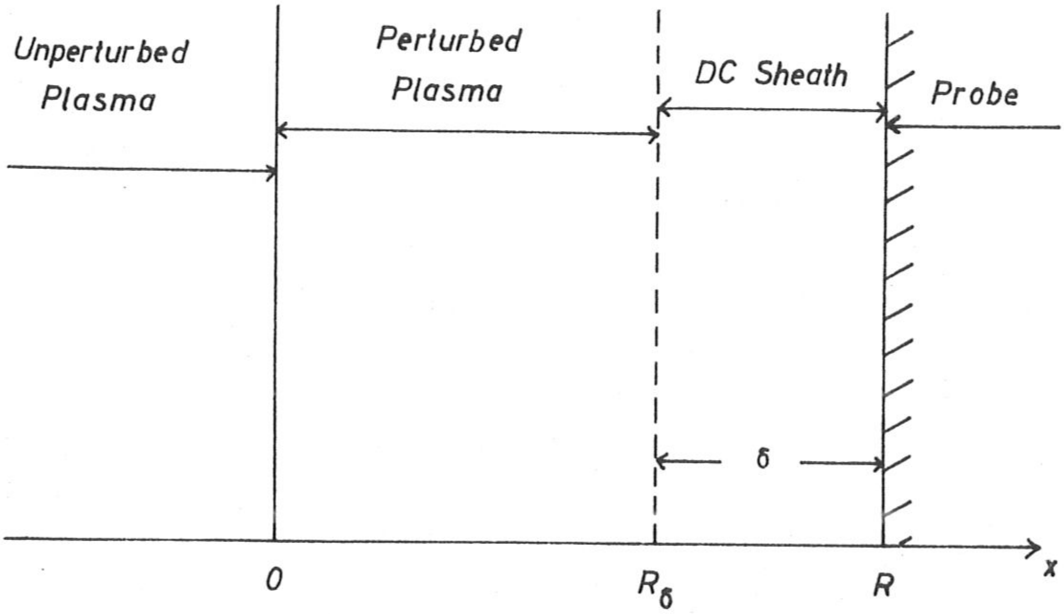
Unperturbed
Plasma
Perturbed
Plasma
DC Sheath
Probe
δ
0
R_δ
R
x

Fig. 4

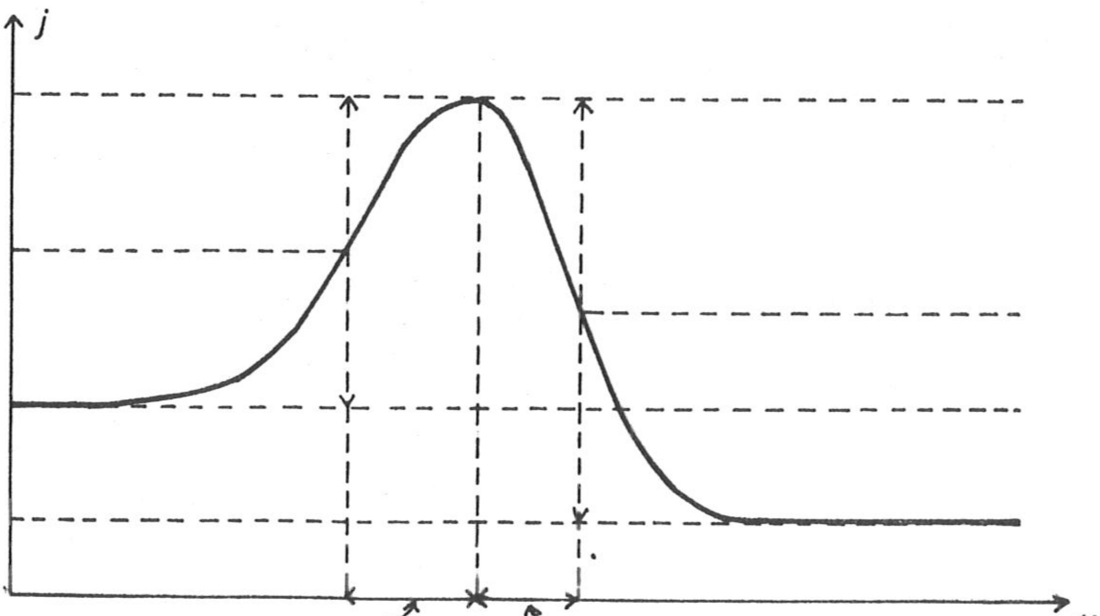
j
ω
$\Delta\omega_L$
$\Delta\omega_H$

Fig. 5

Model 1

$r_D/R = 0,1$

$\nu/\omega_p = 0,6$

$\eta = 3$

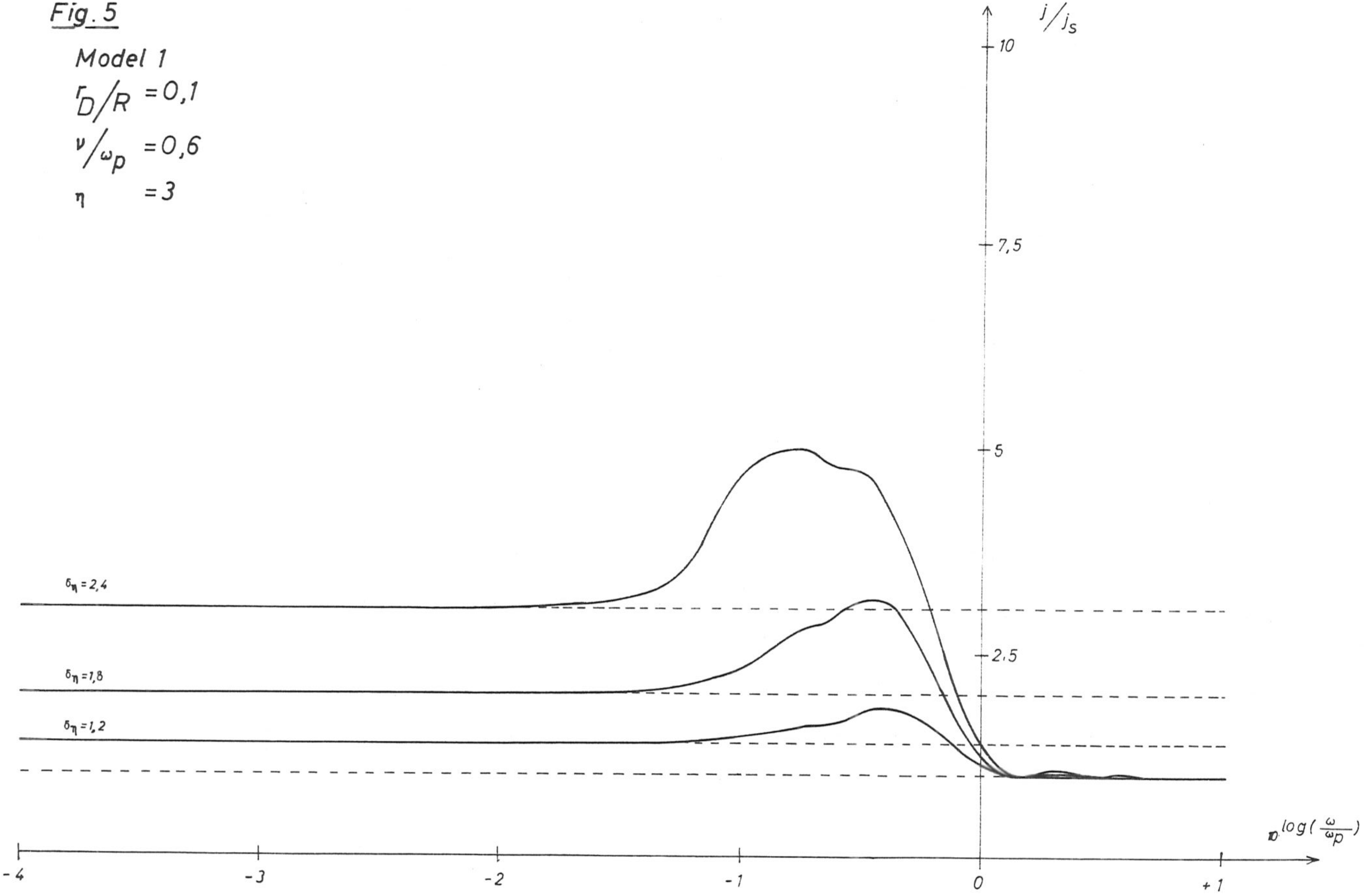

Fig. 6

Model 1

$r_D/R = 0{,}1$

$\nu/\omega_p = 0{,}6$

$\eta = 6$

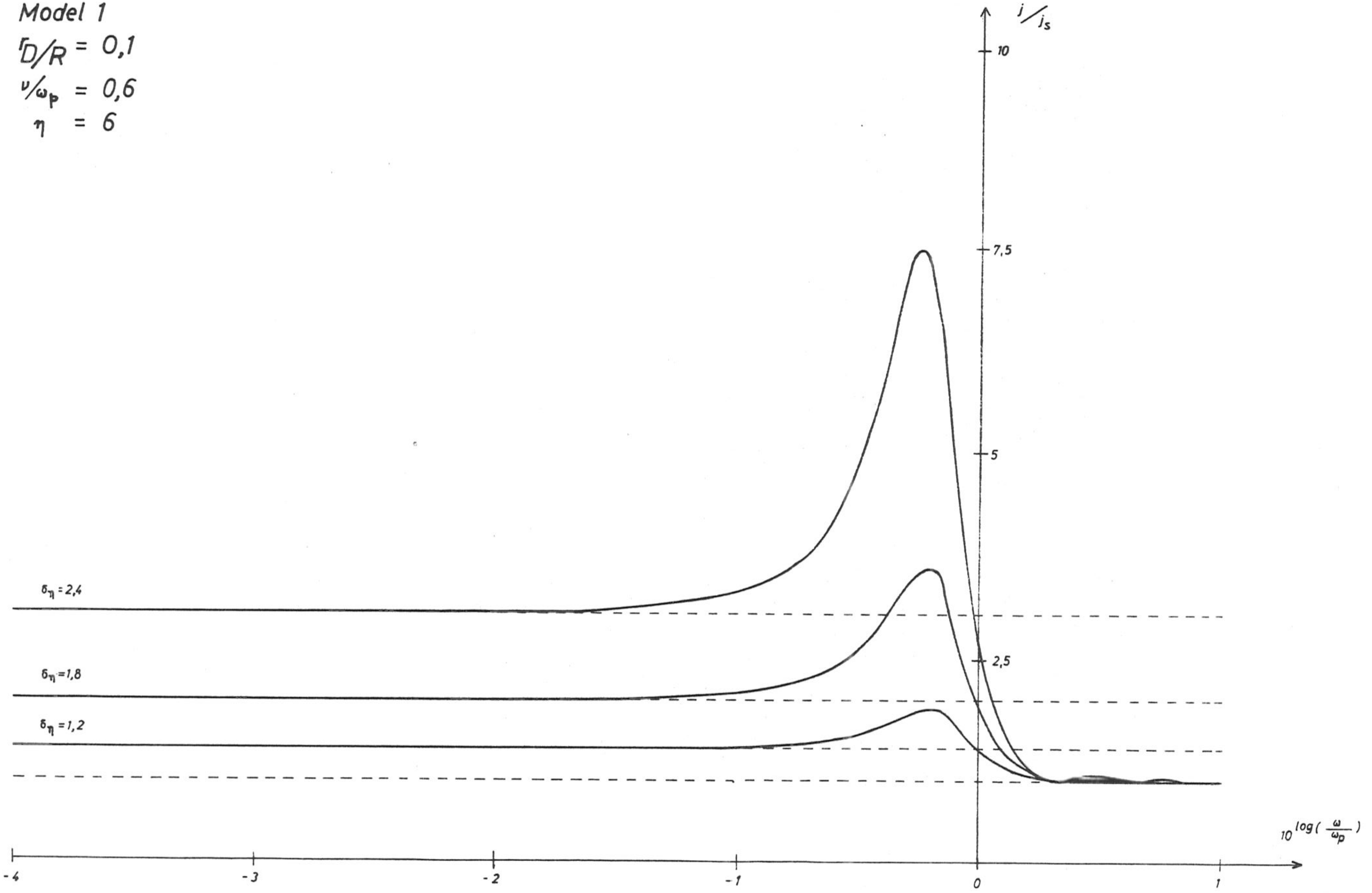

Fig. 7

Model 1

$r_D/R = 0,1$

$\nu/\omega_p = 0,6$

$\eta = 9$

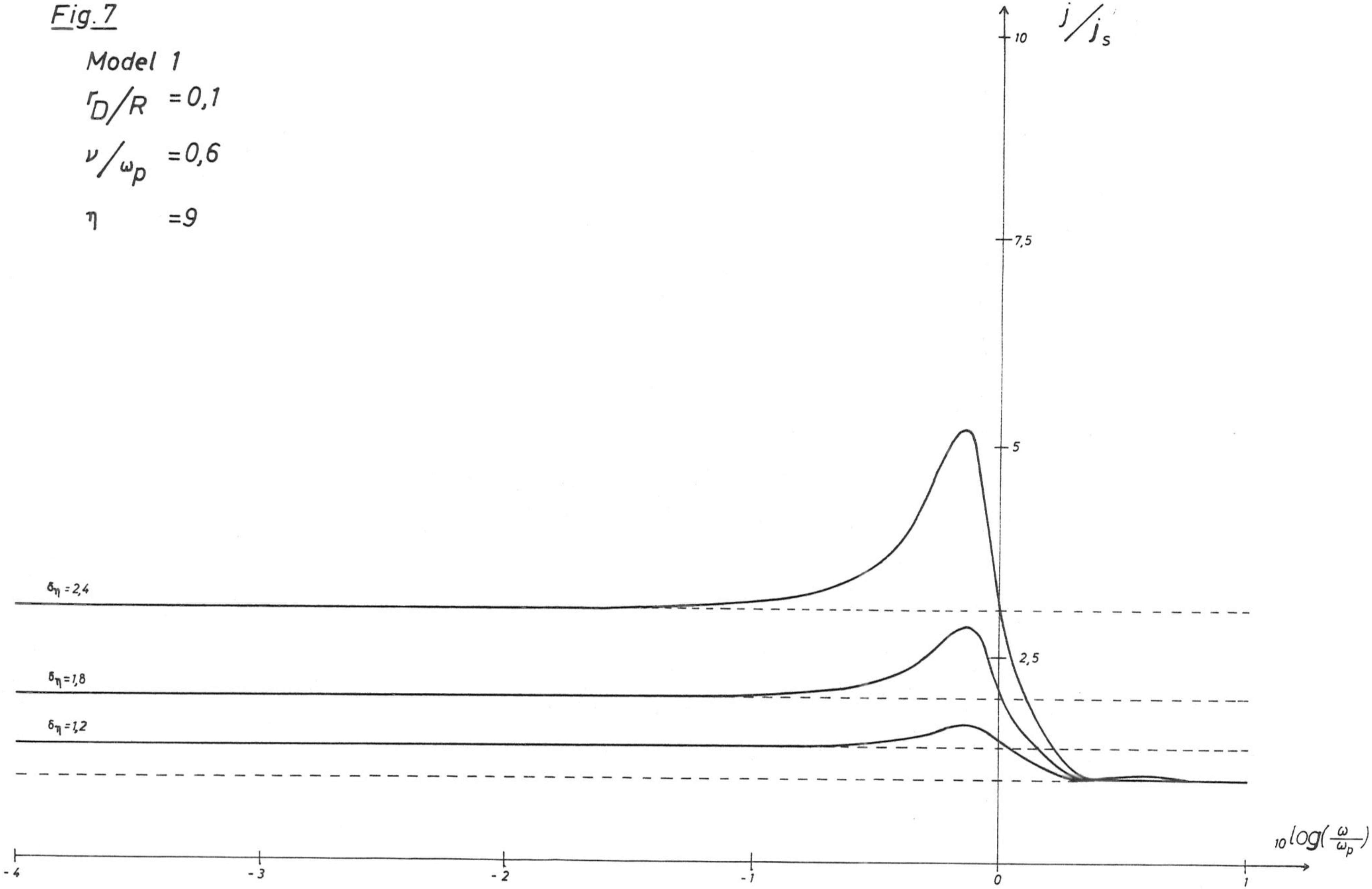

Fig. 8

Model 1

$r_D/R = 0,1$

$\nu/\omega_p = 0,6$

$\eta = 12$

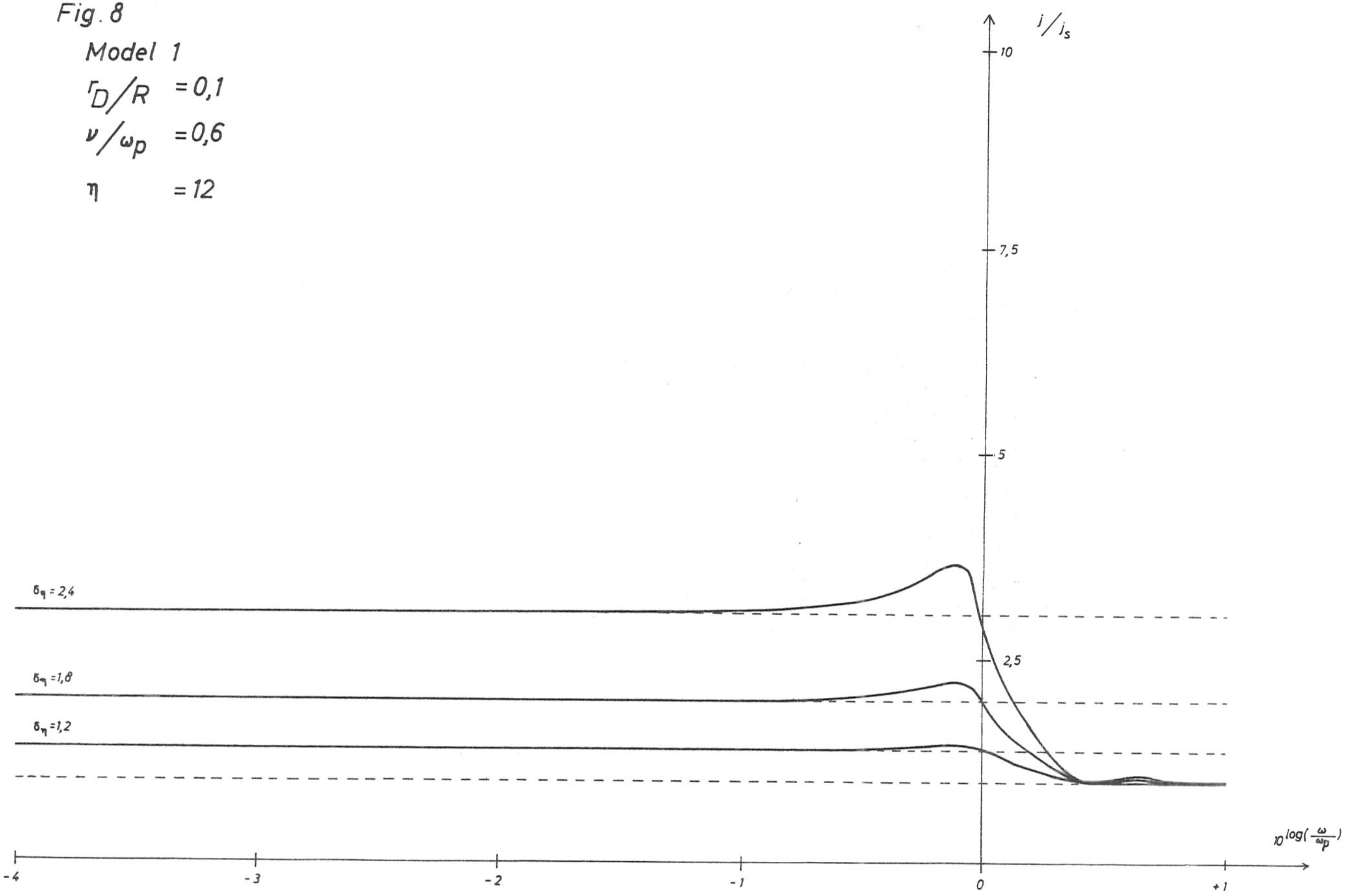

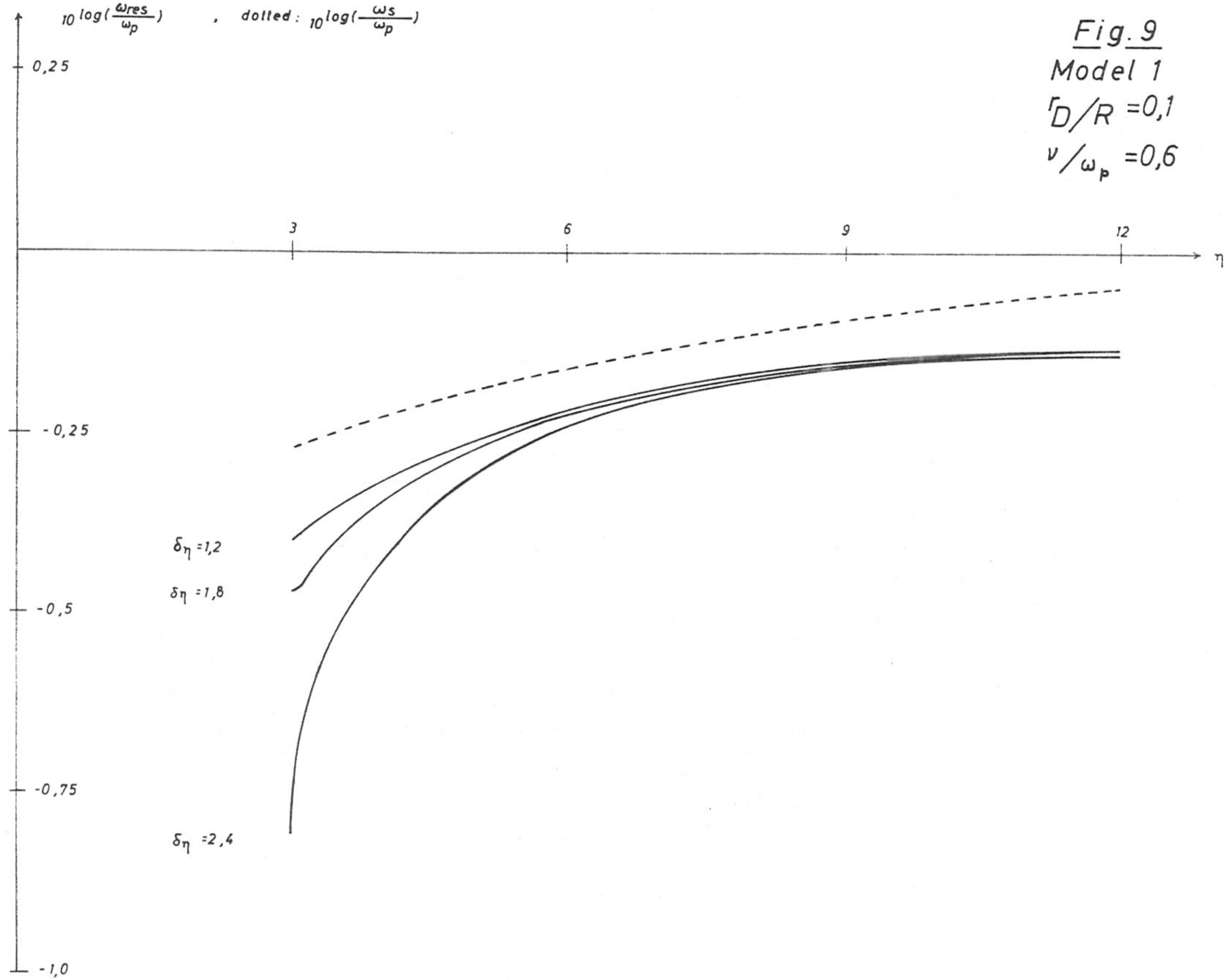

Fig. 9
Model 1
$r_D/R = 0,1$
$\nu/\omega_p = 0,6$

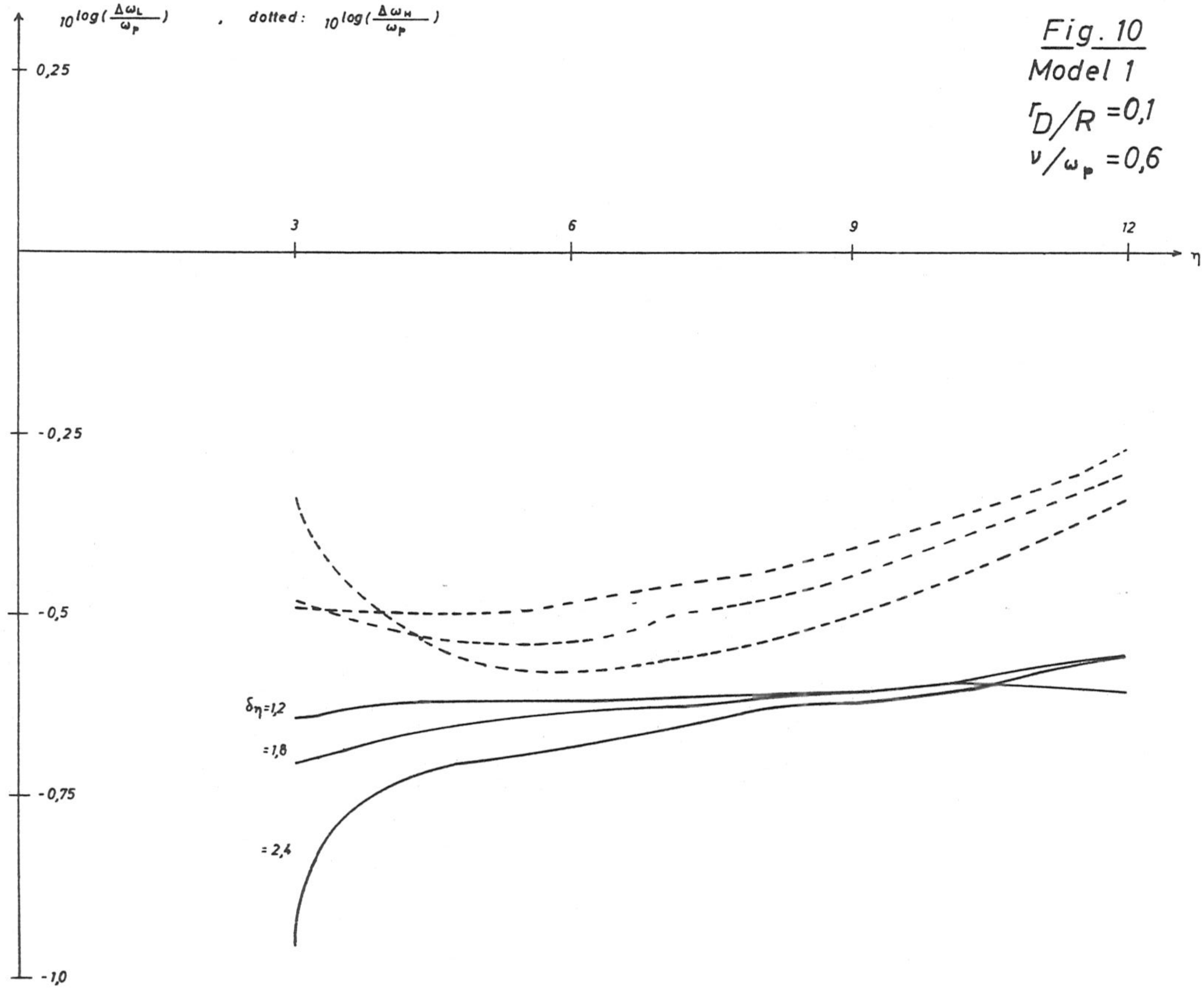

Fig. 10
Model 1
$r_D/R = 0{,}1$
$\nu/\omega_p = 0{,}6$

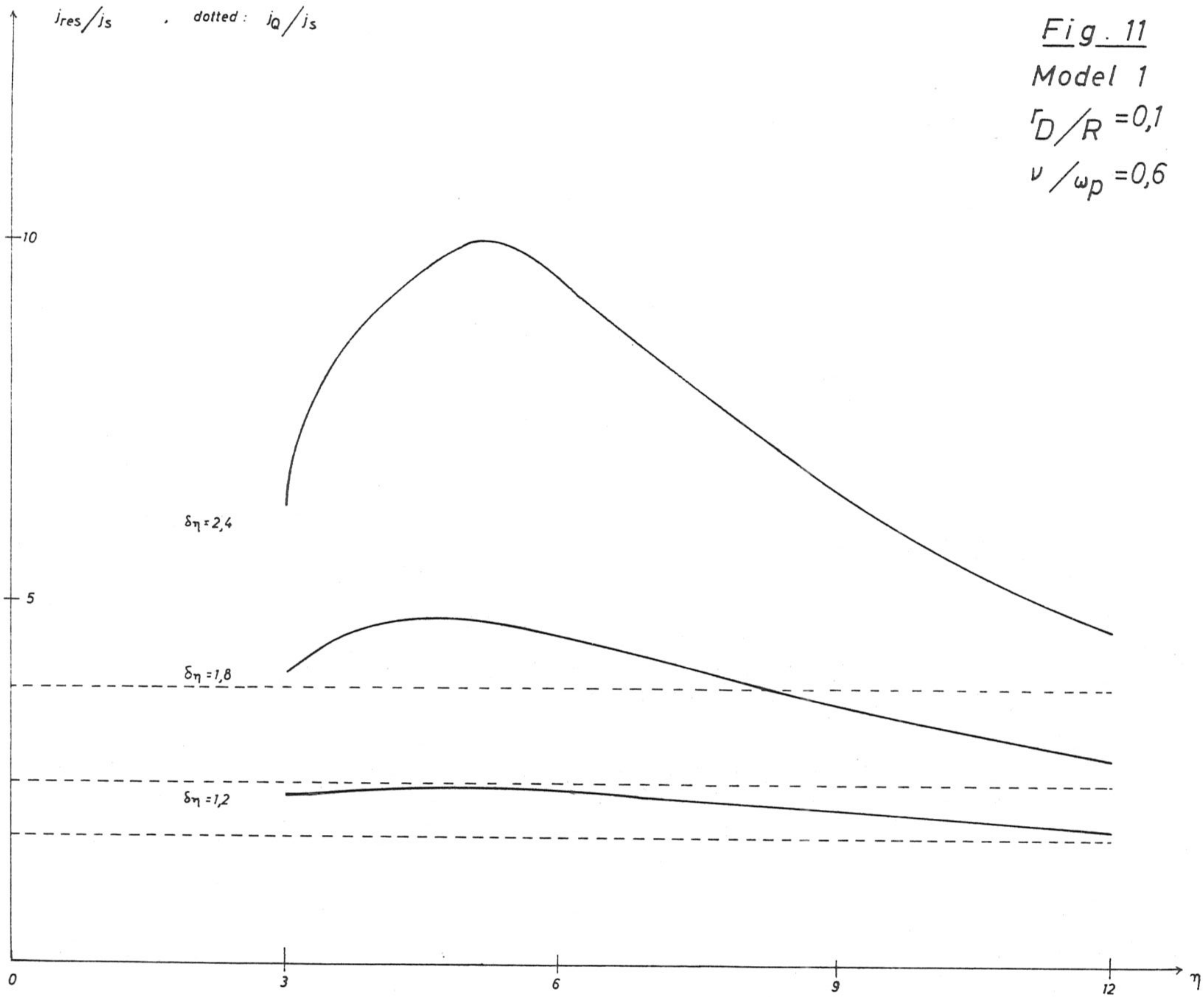

Fig. 11
Model 1
$r_D/R = 0{,}1$
$\nu/\omega_p = 0{,}6$

Fig. 12

Model 2

$r_D/R = 0,1$

$\nu/\omega_p = 0,6$

$\eta = 3$

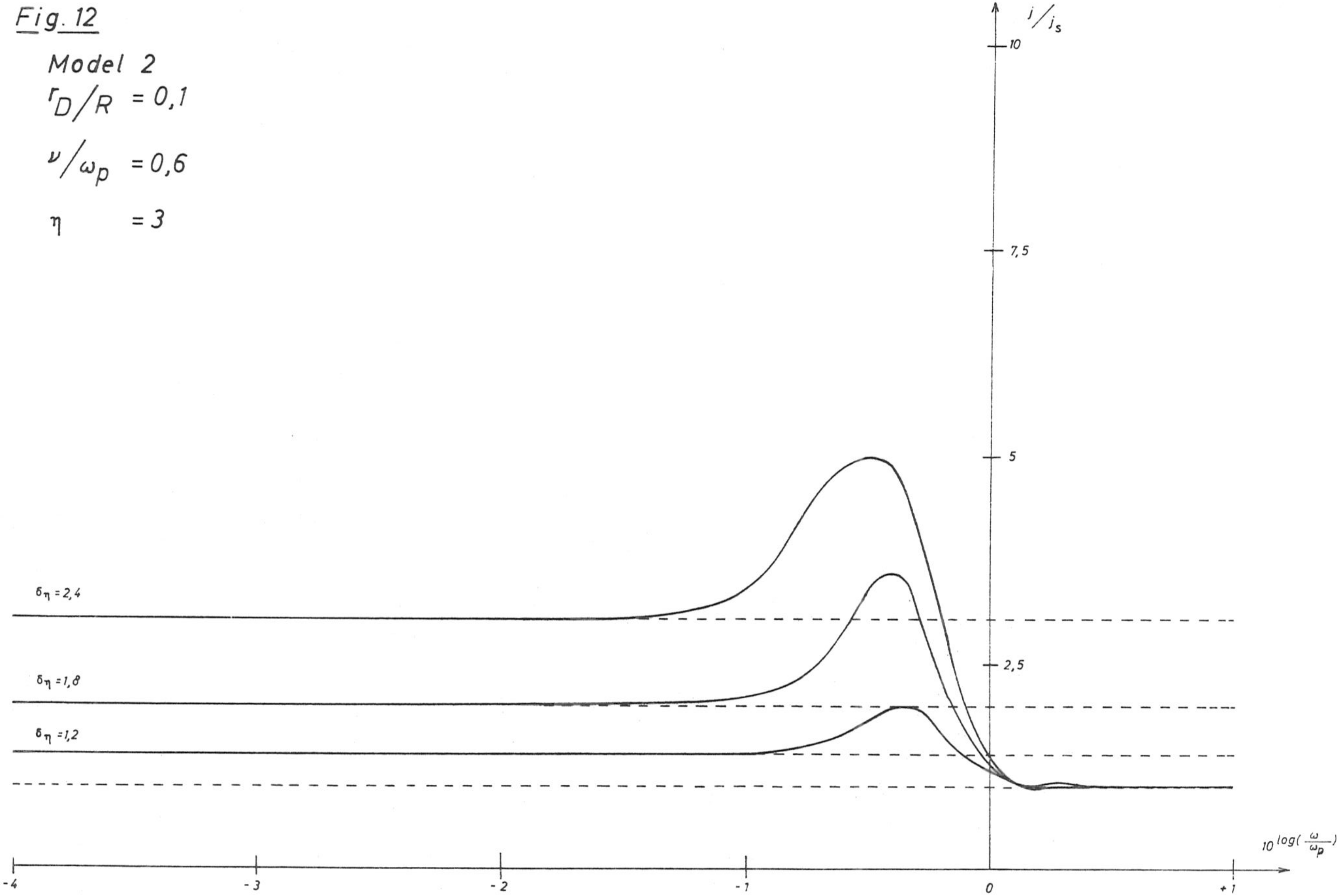

Fig. 13

Model 2

$r_D / R = 0{,}1$

$\nu / \omega_p = 0{,}6$

$\eta = 6$

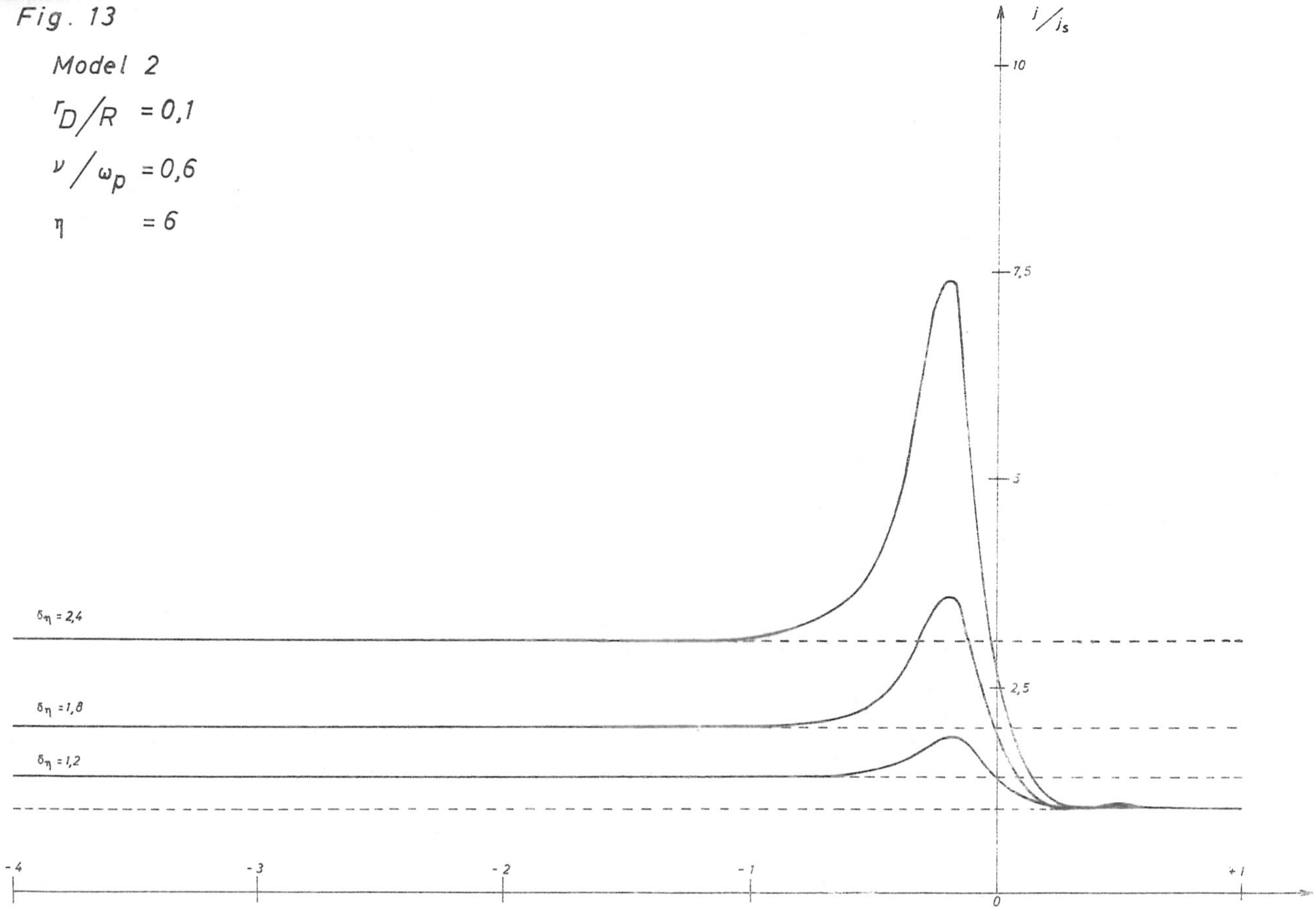

Fig. 14

Model 2

$r_D/R = 0{,}1$

$\nu/\omega_p = 0{,}6$

$\eta = 9$

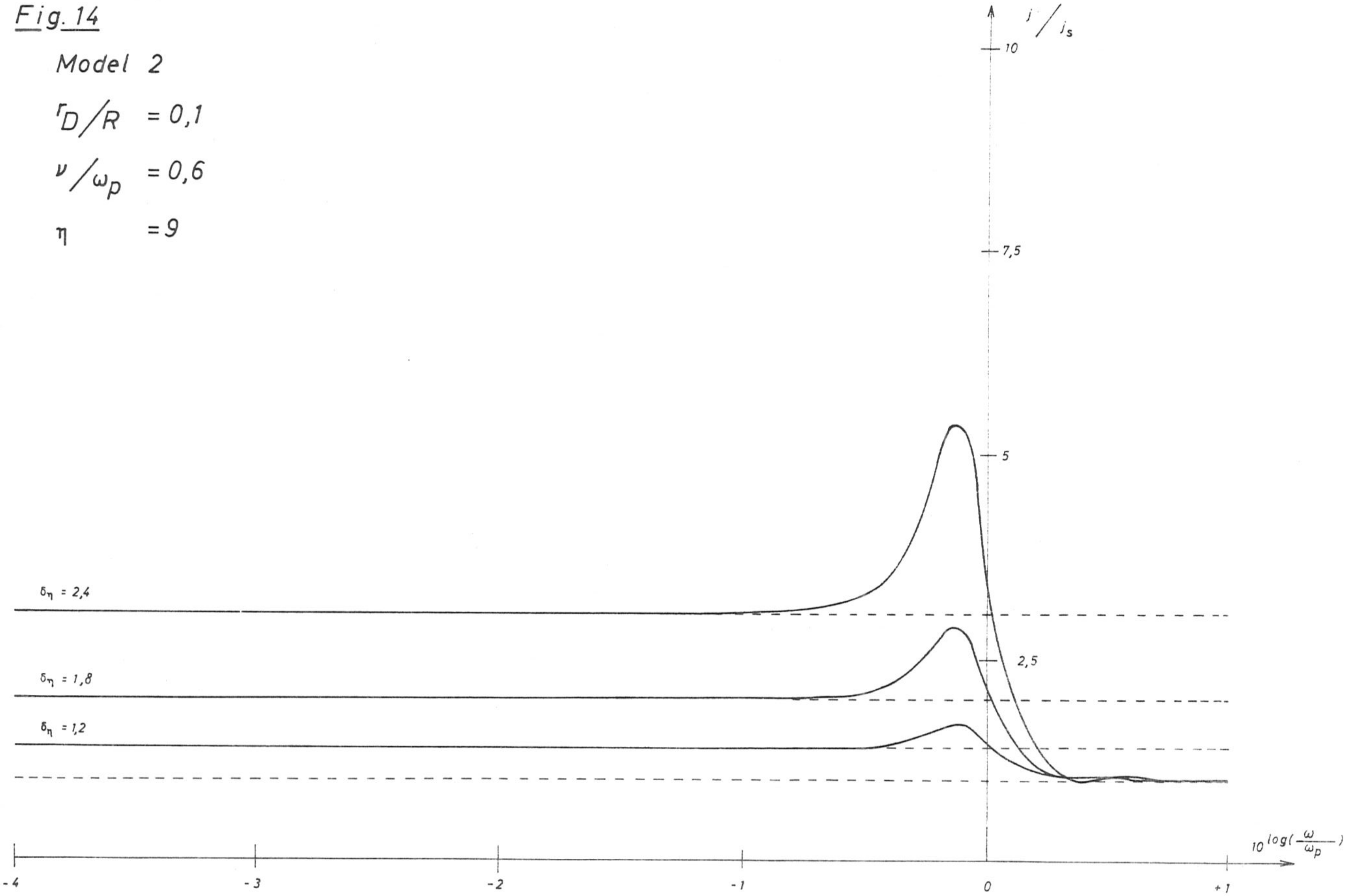

Fig. 15

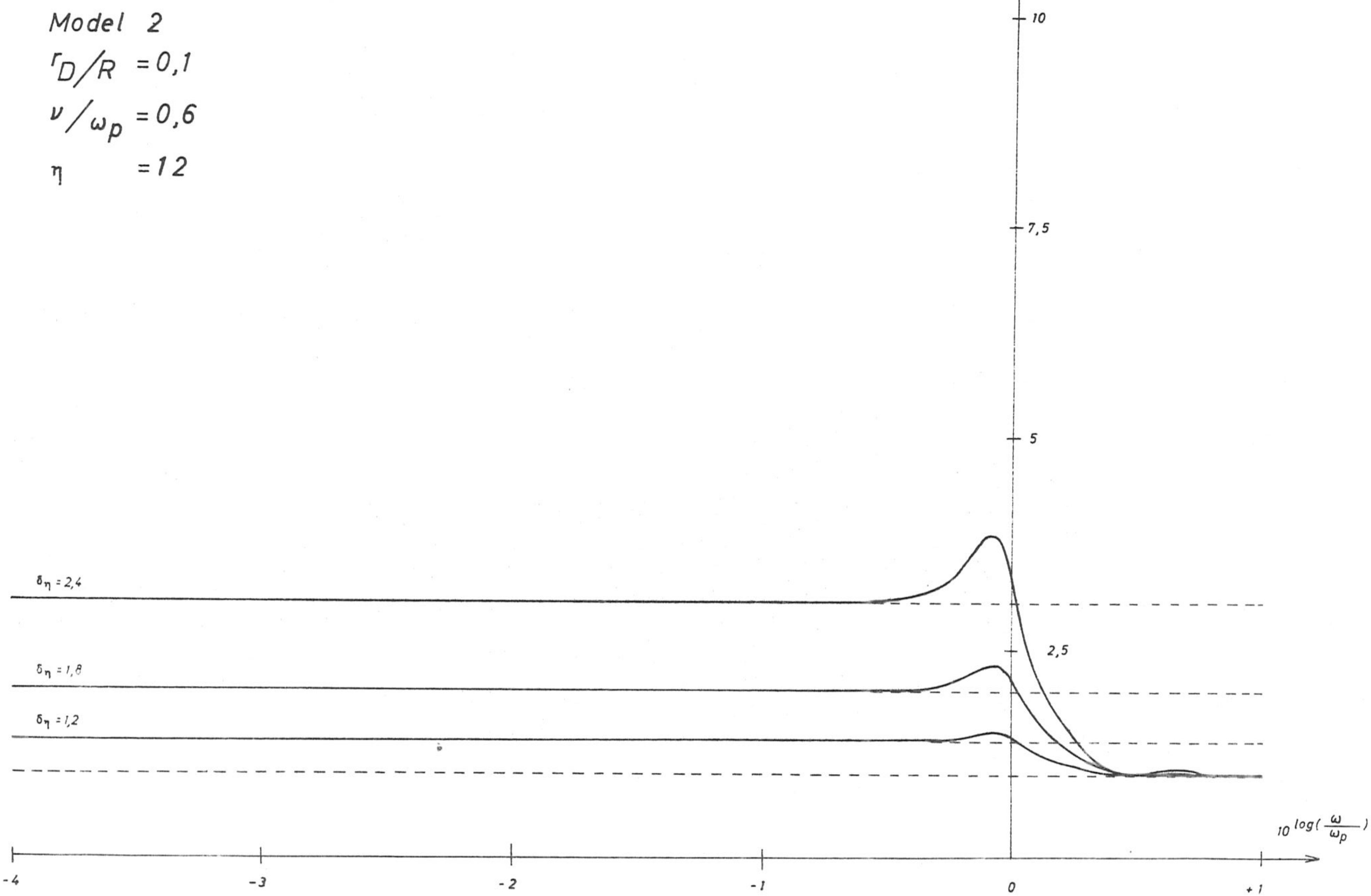

Model 2
$r_D/R = 0,1$
$\nu/\omega_p = 0,6$
$\eta = 12$
j/j_s
10
7,5
5
2,5
$\delta_\eta = 2,4$
$\delta_\eta = 1,8$
$\delta_\eta = 1,2$
$^{10}\log(\frac{\omega}{\omega_p})$
-4
-3
-2
-1
0
+1

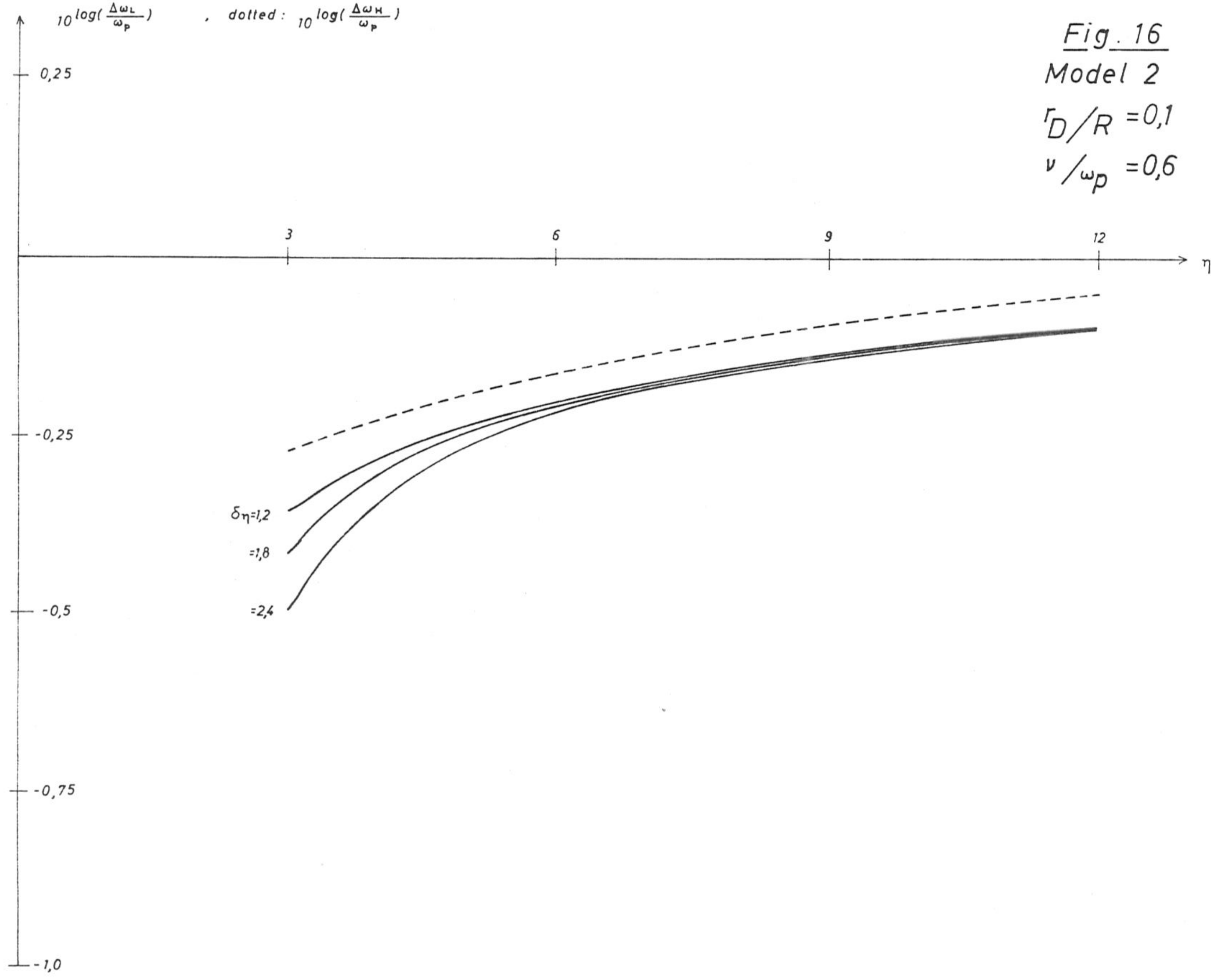

Fig. 16
Model 2
$r_D/R = 0,1$
$\nu/\omega_p = 0,6$

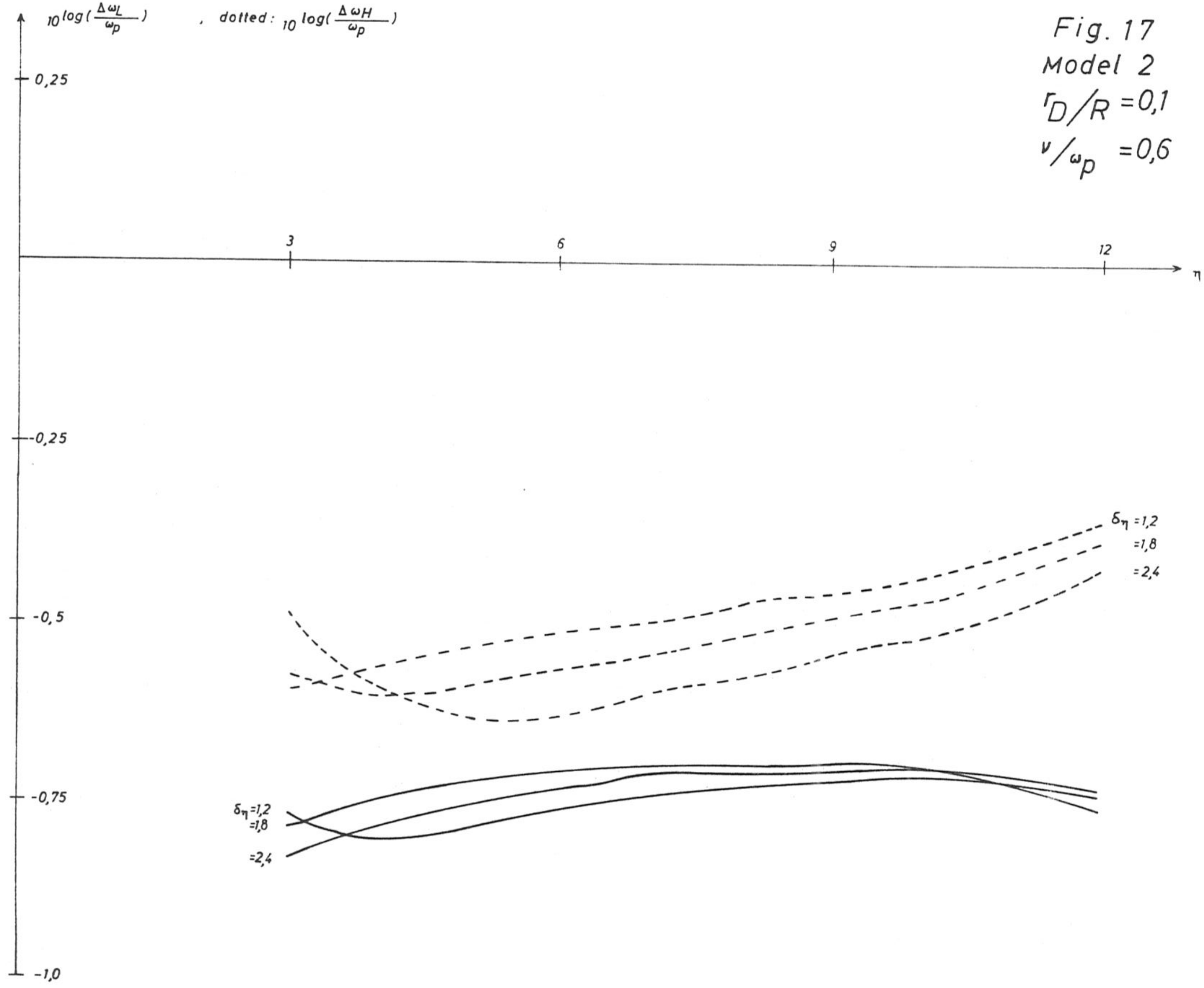

Fig. 17
Model 2
$r_D/R = 0,1$
$\nu/\omega_p = 0,6$

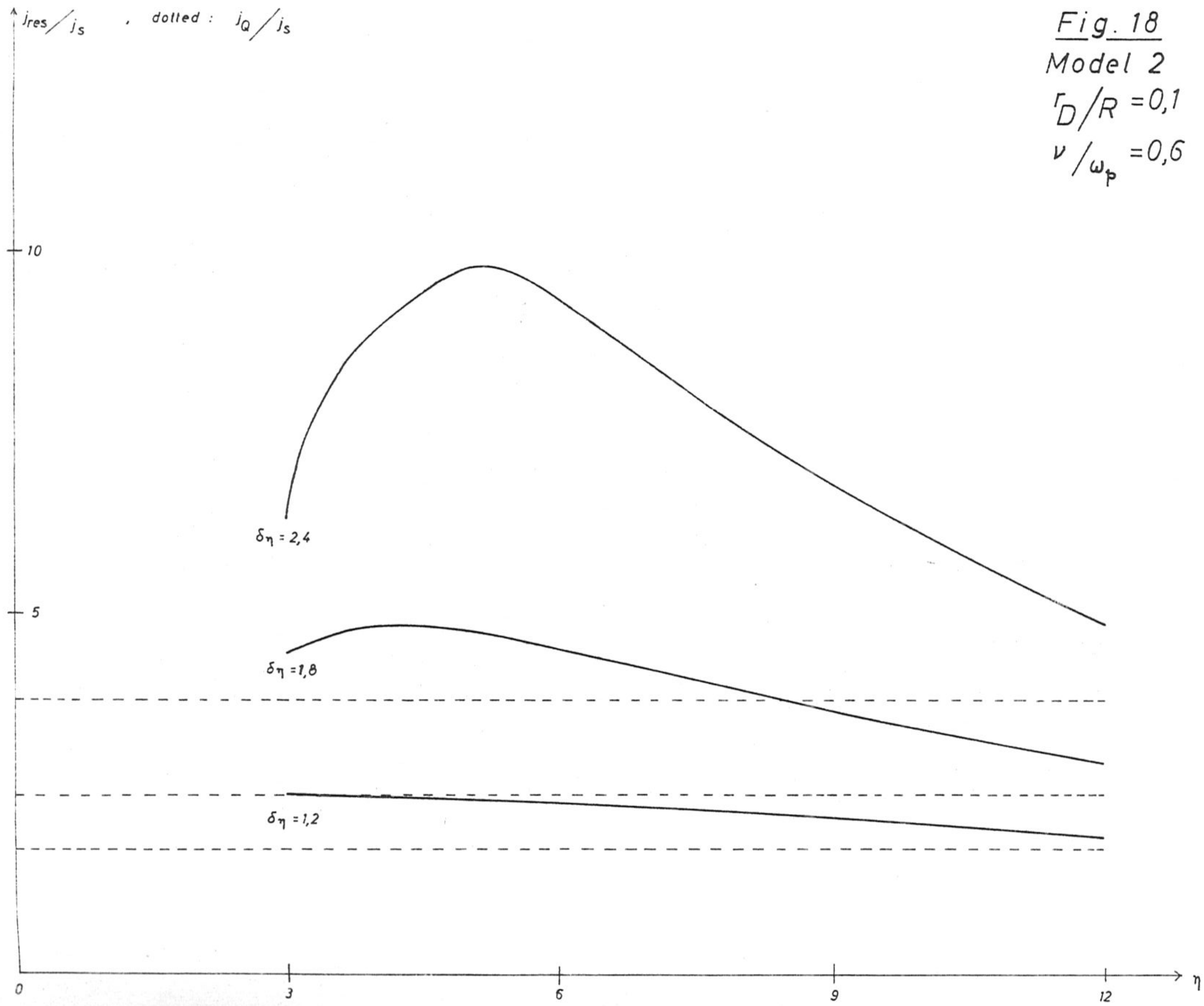

Fig. 18
Model 2
$r_D/R = 0,1$
$\nu/\omega_p = 0,6$